Copper(II) cubanes with a {Cu_4O} core and well defined S = 1 ground state†

A. Escuer,*[a] J. Mayans[a] and M. Font-Bardia[b]

†Department de Quimica Inorgànica i Orgànica and and Institute of Nanoscience and Nanotechnology (IN2UB),, Universitat de Barcelona, Av. Diagonal 645, Barcelona – 08028, Spain
‡Departament de Mineralogia, Cristal·lografia i Dipòsits Minerals and Unitat de Difraccióde R-X, Centre Científic i Tecnològic de la Universitat de Barcelona, Universitat de Barcelona, Solé i Sabarís 1-3, 08028 Barcelona, Spain

Albert Escuer: albert.escuer@ub.edu

ABSTRACT:

The reaction of 2-pyridinemethanol with copper 4-fluorobenzoate has yielded a family of type II cubanes with formula $[Cu_4(pymO)_4(4\text{-F-PhCOO})_3(NO_3)]$ (1), $[Cu_4(pymO)_4(4\text{-F-PhCOO})_4]$ (2) and $[Cu_4(pymO)_4(4\text{-F-PhCOO})_4(H_2O)]$ (3). These systems exhibit an unexpected S = 1 ground state and their magnetic properties have been unambiguously characterized and rationalized as a function of the asymmetry of the $\{Cu_4O_4\}$ cage and Cu–O–Cu bond angles. Analysis of the coupling constants was performed applying new interaction schemes. Magneto-structural correlations have been performed from the analysis of previously reported type II copper cubanes..

Introduciton

Copper cubanes have been classified in structural types as a function of their topology and degree of distortion. Mergehenn and Haase[1] proposed a classification based on the relative distribution of the elongated Cu–O distances in the cube: if the four elongated distances are roughly parallel, the cube can be envisaged as two weakly interacting dimeric subunits (named type I) whereas if the elongated distances are distributed perpendicularly on two opposite faces of the cube (named type II), it can be envisaged to be a folded Cu_4O_4 ring with four weak additional interactions (Scheme 1). More recently, Alvarez et al[.2] made an alternative proposal based on the distribution of the six Cu···Cu distances, with the (2 + 4) and (4 + 2) classes being equivalent to types I and II, respectively, and by adding a new class in which the six Cu···Cu distances are similar, named the (6 + 0) class. The (2 + 4) and (4 + 2) cubes usually corresponds to systems in which the Cu^{II} cations have a square pyramidal or elongated octahedral environment whereas the (6 + 0) cubes should be assigned to the scarce cores with six equivalent faces, in which the coordination polyhedron around the Cu^{II} cations is usually a trigonal bipyramid. Obviously, the magnetic properties of the cubes are strongly dependent on the structure, the (6 + 0) class being closer to a true cube while the type I or (2 + 4) class is closer to two more or less weakly interacting dimers and the type II or (4 + 2) class is more related to a distorted Cu_4 ring.

In all reported cases, dominant anti- or ferromagnetic interactions mediated by the short Cu–O superexchange pathways lead to the $S = 0$ or $S = 2$ typical ground states.

2-Pyridinemethanol (pymOH) and the closely related (*R/S*)-α-methyl-2-pyridinemethanol (MpymOH) ligands are able to generate polynuclear systems linking up to three cations (Scheme 2). Their copper chemistry has been poorly explored and only some dimers,[3] isolated[4] or linked cubanes,[4c,5] single chains[6] and some heterometallic Cu^{II}–Gd^{III} clusters[7] have been reported for pymOH and only one pair of enantiomers[8] have been described for (*R/S*)-MpymOH. Our initial target was to explore the reactivity of these ligands in carboxylate-copper chemistry but unfortunately unambiguous characterization was only possible for pymOH derivatives.

In this work we report the syntheses and characterization of three new cubanes with a Cu_4O_4 core belonging to the (4 + 2) class, obtained from the reaction of copper(II) 4-fluorobenzoate and 2-pyridylmethanol (pymOH) with formulas $[Cu_4(pymO)_4(4\text{-F-PhCOO})_3(NO_3)]$ (1), $[Cu_4(pymO)_4(4\text{-F-PhCOO})4]$ (2) and $[Cu_4(pymO)_4(4\text{-F-PhCOO})_4(H_2O)]\cdot 0.5MeOH \cdot 0.25H2O$ ($3\cdot 0.5MeOH \cdot 0.25H_2O$). Magnetic susceptibility and magnetization measurements prove that these systems possess a well isolated $S = 1$ ground state. This unique property has been rationalized as a function of the cage bond parameters. We also report a general study of the magnetic response of the previously reported (4 + 2) class cubes and a critical analysis of the models usually applied to fit the magnetic data.

Experimental

Materials and methods

The $Cu(4\text{-F-PhCOO})_2$ starting reagent was synthesized in typical yields >70% mixing equimolecular amounts of aqueous solutions of $Cu(NO_3)_2{\cdot}6H_2O$ and Na(4-F-PhCOO) salts. The copper carboxylate was collected *via* filtration and washed with cold water. Samples for analysis were gently dried to remove volatile solvents. The yield for 1–3 was around 25% of well formed crystals which were employed for instrumental measurements.

IR spectra (4000–400 cm^{-1}) were recorded using a Bruker IFS-125 FT-IR spectrometer with samples prepared as KBr pellets. Variable-temperature magnetic studies were performed using a MPMS-5 Quantum Design magnetometer operating at 0.03 T in the 300–2.0 K range. Diamagnetic corrections were applied to the observed paramagnetic susceptibility using Pascal's constants.

Energy levels plotted in Fig. 4b–d and those in Fig. 6 have been calculated for an arbitrary J_2 value of -50 cm^{-1}.

Single-crystal X-ray crystallography

Blue prism-like specimens of approximate dimensions 0.196 mm × 0.336 mm × 0.522 mm (1), 0.082 mm × 0.168 mm × 0.227 mm (2) and 0.390 mm × 0.397 mm × 0.508 mm (3) were used for X-ray crystallographic analysis. The X-ray intensity data were measured on a D8 Venture system equipped with a multilayer monochromator and a Mo microfocus (λ = 0.71073 Å). The frames were integrated with the Bruker SAINT software package using a narrow-frame algorithm. The final cell constants were based upon the refinement of the XYZ-centroids of reflections above 20 σ(I). Data were corrected for absorption effects using the multi-scan method (SADABS). The structures were solved using the Bruker SHELXTL Software Package, and refined using SHELXL.[9] Details of crystal data, collection and refinement for 1–3 are summarized in Table 1. Analyses of the structures and plots for publication were performed with the Ortep3[10] and POVRAY programs.

Synthetic procedure

$[Cu_4(pymO)_4(4\text{-F-PhCOO})_3(NO_3)]$ (1). A few crystals of complex 1 were initially obtained from a $Cu(4\text{-F-PhCOO})_2$ starting reagent contaminated with nitrates. In light of the structural results, the synthesis was repeated by dissolving $Cu(4\text{-F-PhCOO})_2$ and $Cu(NO_3)_2{\cdot}6H_2O$ in a 3 : 1 ratio (0.375 mmol, 0.128 g : 0.125 mmol, 0.037 g) in methanol (5 mL) and the ligand pymOH in 5 mL of acetonitrile. Both solutions were mixed and stirred for three hours.

Complex 1 crystallizes as blue crystals *via* vapour diffusion with diethyl ether. Anal. Calcd for $C_{45}H_{36}Cu_4F_3N_5O_{13}$ (1): C, 46.35; H, 3.11; N, 6.01%. Found: C, 46.92; H, 3.4; N, 5.88%. Relevant IR bands: 3440 (s, broad), 3077(w), 2835 (w), 1620(s), 1580(s), 1506(s), 1440(s), 1360(s), 1310 (s), 1210(w), 1150(w), 1050(s), 860(w), 785(w), 760(w), 630(w) cm^{-1}.

$[Cu_4(pymO)_4(4\text{-F-PhCOO})_4]$ (2). $Cu(4\text{-F-PhCOO})_2$ (0.5 mmol, 0.170 g) was dissolved in methanol (5 mL) and the ligand pymOH was dissolved in 5 mL of acetonitrile. Both solutions were mixed and stirred for three hours. Slow evaporation of the resulting solution yields complex 2 as blue crystals. Anal. Calcd

for $C_{52}H_{40}Cu_4F_4N_4O_{12}$ (2): C, 50.24; H, 3.24; N, 4.51%. Found: C, 49.32; H, 3.10; N, 4.31%. Relevant IR bands: 3440 (s, broad), 3077(w), 2835 (w), 1620(s), 1440 (w), 1400(s), 1360(w), 1250(w), 1210(w), 1150(w), 985(w), 630(w), 480(w), 411(w) cm^{-1}.

$[Cu_4(pymO)_4(4\text{-F-PhCOO})_4]\cdot 0.5MeOH\cdot 0.25H_2O$ ($3\cdot 0.5MeOH\cdot 0.25\text{-}H_2O$). $Cu(4\text{-F-PhCOO})_2$ (0.5 mmol, 0.170 g) was dissolved in methanol (5 mL). The ligands pymOH (0.75 mmol, 0.081 g) and (S-pyeOH) (0.25 mmol, 0.035 g) were dissolved in acetonitrile (5 mL). The mixture of both solutions was stirred for three hours, filtered and layered with diethyl ether. Well formed blue crystals suitable for X-Ray analysis grew after two weeks. Anal. Calcd for $C_{52.5}H_{44.5}Cu_4F_4N_4O_{13.75}$ ($3\cdot 3\cdot 0.5MeOH\cdot 0.25H2O$): C, 49.20; H, 3.50; N, 4.37%. Found: C, 49.73; H, 3.41; N, 4.16%. Relevant IR bands: ν = 3440 (s, broad), 3160(w) 2835 (w), 1610(s), 1550(s), 1400(s), 1210(s), 1080 (s), 860(s), 780(s), 618(s), 530(w) cm^{-1}.

Results and discussion

Structural description

$[Cu_4(pymO)_4(4\text{-F-PhCOO})_3(NO_3)]$ (1). The molecular structure consists of isolated cubanes with a $\{Cu_4O_4\}$ core. A view of the structure is shown in Fig. 1 and the main bond parameters are summarized in Table 2. One pymO− ligand is coordinated to each copper cation, providing the four μ_3-alcoxo corners of the cube. The pymO− ligands are placed roughly perpendicular to two opposite faces of the cube whereas three of the remainder four faces are occupied by the three bidentate carboxylates. The nitrate anion acts as monodentate ligand, coordinated to Cu4. Cu2 shows a square pyramidal $CuNO_4$ environment whereas Cu(1,3,4) exhibit an axially elongated octahedral $CuNO_5$ coordination polyhedron. The elongated axial bond distances involve one Cu–O cage bond for each copper cation and one Cu–O bond with one O-carboxylate or O-nitrate for Cu(1,2,4). The equatorial bond distances are in the short 2.000–1.905 Å range whereas the axial Cu–O bond distances are relatively large, ranging between 2.344(3)–2.697(3) Å.

$[Cu_4(pymO)_4(4\text{-F-PhCOO})_4]$ (2). A view of the structure is shown in Fig. 2 and the main bond parameters are summarized in Table 2. The structure is very similar to 1 but in this case the nitrate ligand has been substituted by a fourth carboxylate. In this case two carboxylates act as bidentate ligands coordinated to the neighbor {Cu1/O4/Cu4/O10} and {Cu1/O10/ Cu3/O1} faces whereas the other two carboxylates act as monodentate ligands coordinating Cu2 and Cu3. Cu1 and Cu4 show an elongated octahedron coordination polyhedron whereas Cu2 and Cu3 exhibit a square pyramidal environment. The core of the cube is more distorted than complex 1 as is reflected in the large Cu4–O7 distance of 2.962(7) Å or the Cu4–O4–Cu2 bond angle of 120.1(3)°.

$[Cu_4(\ pymO)_4(4\text{-F-PhCOO})_4(H_2O)]\cdot 3\cdot 0.5MeOH\cdot 0.25H2O$ ($3\cdot 3\cdot 0.5MeOH\cdot 0.25H_2O$). A view of the structure is shown in Fig. 3 and the main bond parameters are summarized in Table 2. The structure of 3 is closely related to compound 2 but now there is an additional water molecule coordinated to Cu2, which turns to be hexacoordinated. The coordinated water molecule establishes two strong H-bonds with the noncoordinated O6 and O12 atoms belonging to the monodentate carboxylates and also interacts with the crystallization water molecule. O6···O3w and O12···O3w distances are 2.685(3) and 2.780(2) Å respectively. The presence of this new ligand on Cu2 increase the distance between the monodentate carboxylates and as a consequence, displaces Cu4 with the concomitant increase of the Cu4–O7 distance (up to 3.253 Å) and the Cu2–O4–Cu4 bond angle, which reaches 124.32(6)°. As can be seen in Table 2, the three cubes are quite similar in their general trends, increasing the distortion of the cage from the least (1) to most distorted (3) cube.

Spin levels and ground state for the Cu4 (4 + 2) cubane topology

The magnetic properties for the (4 + 2) copper cubane topology have been widely studied via DFT calculations[2,11] and all studied cases lead to the S = 0 or S = 2 ground state. As can be expected, it was also stated that the axial-equatorial interactions involving often very large Cu–O distances (on two elongated opposite faces, Scheme 1) must always be weak.2 Surprisingly, the susceptibility measurements performed for complexes 1–3 clearly suggest an unprecedented “anomalous” intermediate spin ground state S = 1 (see further magnetic properties discussion), apparently incompatible with a Cu^{II} cubane topology.

To have a clear picture of the magnetic properties of all previously reported cubanes with a (4 + 2) shape, a search in the CCDC database was performed and 119 entries were obtained for Cu^{II} cubes with four elongated Cu–O bonds larger than 2.100 Å as the only restraint. Cubes for which the complete magnetic analysis was not reported or the coordination polyhedron around the Cu^{II} cations was a trigonal bypyramid were discarded from this study. The magnetic data for the 43 (4 + 2) Cu^{II} cubes with reported magnetic data and a square pyramidal or elongated octahedral environment around the Cu^{II} cations are summarized in Table 3.

The next step was to check which models were applied to fit the experimental data and up to five models were found to describe the magnetic response of these systems (Scheme 3).

Despite the evidence that the superexchange interaction mediated by the opposite faces with exclusively axial–equatorial (Jahn–Teller) pathways is usually poorly effective in comparison with the four faces with equatorial–equatorial pathways,[2,11] some coupling constants analysis were performed assuming a regular model (Scheme 3, model (6) and Table 3), for which the corresponding Hamiltonian is:

$$H = -J_1(S_1 \cdot S_2 + S_1 \cdot S_3 + S_1 \cdot S_4 + S_2 \cdot S_3 + S_2 \cdot S_4 + S_3 \cdot S_4) \quad (1)$$

On the other hand, the magnetic properties for most of the reported systems were calculated with the (2:4) or (0:4) models (Scheme 3 and Table 3) for which the Hamiltonians are:

$$H = -J_1(S_1 \cdot S_2 + S_3 \cdot S_4) - -J_2(S_1 \cdot S_3 + S_1 \cdot S_4 + S_2 \cdot S_3 + S_2 \cdot S_4) \quad (2)$$

$$H = -J_2(S_1 \cdot S_3 + S_1 \cdot S_4 + S_2 \cdot S_3 + S_2 \cdot S_4) \quad (3)$$

For a reduced number of asymmetric cubes, models taking into account different interactions for each pair of opposite faces of the cube were applied (models (0:2:2) and (2:2:2), Scheme 3 and Table 3), applying the Hamiltonians:

$$H = -J_2(S_1 \cdot S_3 + S_2 \cdot S_4) - -J_3(S_2 \cdot S_3 + S_1 \cdot S_4) \quad (4)$$

$$H = -J_1(S_1 \cdot S_2 + S_3 \cdot S_4) - -J_2(S_1 \cdot S_3 + S_2 \cdot S_4) - J_3(S_2 \cdot S_3 + S_1 \cdot S_4) \quad (5)$$

Hamiltonians (3) and (4) are the limit of (2) and (5) when J_1 was neglected assuming $J_2, J_3 \gg J_1$. The reported ground state for all cubes applying Hamiltonians (1)–(5) is systematically S = 0 for negative $J_{2,3}$ values or S = 2 for positive ones. This experimental feature can be easily rationalized plotting the energy of the six spin levels of the cube (one $S = 2$, three $S = 1$ and two $S = 0$), as a function of the coupling constant.

If we assume that the interaction between the copper centers through the elongated (Jahn–Teller) faces are negligible and the other four interactions are identical, model (0:4) and Hamiltonian (3), we obtain the spin level distribution shown in Fig. 4a, which evidences that $S = 0$ and $S = 2$ are the only possible

ground states as a function of the sign of J_2. If we take into account the elongated faces, model (2:4) and Hamiltonian (2), we realize that for a dominant antiferromagnetic interaction J_2 the ground state is always $S = 0$ (the first $S = 1$ excited state has the same slope) and for a positive sign of J_2, the ground state can switch from $S = 2$ to $S = 0$ for J_2/J_1 ratios lower than −0.5, Fig. 4b and c respectively).

In a few cases, the fit of the experimental data was performed assuming a set of two or three J values for opposite faces of the cubes. Neglecting the interaction mediated by the opposite elongated faces, Scheme (0:2:2) and Hamiltonian (4), we realize that if one of the interactions is antiferromagnetic then $S = 0$ is the ground state for any positive or negative J_2/J_3 ratio (Fig. 4d). As in the (0:4) case, the addition of the weak interactions mediated by the elongated faces, model (2:2:2), only produces very small changes in the energy of the spin levels.

The above calculations exclude these models to analyse compounds 1–3 and then, the origin of their intermediate ground state must be found in other structural facts, neglected until now. The dependence of the magnitude and the sign of the coupling constants as a function of the Cu–O–Cu bond angle has been demonstrated via theoretical calculations and has been the preferred parameter to correlate the magnetic properties.[2,11] The Cu–O–Cu bond angles involved in equatorial–equatorial bridges for the (4 + 2) class of cubes (Fig. 5) take values comprised between 100°–115°, being exceptional to find Cu–O–Cu bond angles below or above these limits. The border between the ferromagnetic–antiferromagnetic response is unclear because it can depend on the characteristics of the bridging ligand that provides the μ^3-O linkage among other factors[2] but, always assuming that there are compounds out of the rule, around 108° is a roughly reasonable limit. As general rule, copper cubanes with these four Cu–O–Cu bond angles clearly lower than 108° tend to be ferromagnetic with a $S = 2$ ground state and those with these bond angles clearly larger than 108° tend to be antiferromagnetic with a $S = 0$ ground state (ESI, Table S1†). In light of these previous data, the detailed analysis of the structures of complexes 1–3 unveils an uncommon feature: the three cages are very asymmetric as a consequence of the coordination of the bidentate carboxylates on the *contiguous* faces. As a consequence, the Cu–O–Cu bond angles involving short Cu–O distances are also more similar on the *contiguous* faces instead of the *opposite* faces as it is common (Table 2). Taking the parameters defined in Fig. 5 as a reference, complex 1 has one large δ bond angle of 112.2°, two short α and β of 100.3° and 102.6° and one intermediate γ of 108.7°. The Cu–O–Cu bond angles for complexes 2 and 3 exhibit two large *contiguous* α and δ angles (110.9°/120.1° and 110.8°/124.4°) and two short β and γ Cu–O–Cu bond angles (101.5°/104.3° and 100.8°/104.2°).

In basis to these structural parameters we attempted the analysis of the energy of the spin levels for the new models plotted in Scheme 4, which describe the interactions as three similar and one different interaction, (0:1:3) model, and two similar interactions on *contiguous* faces, (0:2:2c) model. The corresponding Hamiltonians are:

$$H = -J_2(S_1 \cdot S_4) - J_3(S_1 \cdot S_3 + S_2 \cdot S_3 + S_2 \cdot S_4) \quad (6)$$

$$H = -J_2(S_1 \cdot S_3 + S_1 \cdot S_4)) - J_3(S_2 \cdot S_3 + S_2 \cdot S_4) \quad (7)$$

The plots of the energies of the six spin levels of the cubane topology for these models are shown in Fig. 6. Obviously, if the sign of both the J_2 and J_3 constants is the same, the ground states will be newly $S = 0$ or 2. However, by forming these plots we realize that for the (0:1:3) model $S = 2$ is the ground state if the $-J_3/J_2$ ratio is lower than 1/3 but one of the $S = 1$ spin levels becomes clearly the ground state for larger ratios. Equally for the (0:2:2c) model, for negative J_3/J_2 ratios (i.e. different sign for the two coupling constants) one well isolated $S = 1$ spin level becomes the ground state.

Magnetic properties

χMT vs. T plots for 1–3 are shown in Fig. 7. χMT at room temperature for 1 is 1.86 cm3 $Kmol^{-1}$. Upon cooling, the χMT value decreases continuously down to a plateau value of 1.18 cm^3 $Kmol^{-1}$ around 12 K. Below this temperature $\chi_M T$ raises slightly to decrease finally to 1.12 cm^3 $Kmol^{-1}$ at 2 K. Complexes 2 and 3 exhibit $\chi_M T$ values of 1.55 and 1.51 cm^3 $Kmol^{-1}$ at room temperature. For decreasing temperatures, the $\chi_M T$ value decreases continuously down to a well defined minimum of 1.08 cm^3 $Kmol^{-1}$ at 60 K for 2 and 70 K for 3. At low temperature, the $\chi_M T$ value slightly increases prior to the final decrease to and 1.07 and 1.16 cm^3 $Kmol^{-1}$ at 2 K.

According the crystallographic data and the above proposed models, the susceptibility data was fitted with the PHI program12 applying the (0:1:3) model for 1 (Scheme 4, Hamiltonian (6)) and (0:2:2c) model (Scheme 4, Hamiltonian (7)) for 2 and 3. R quality factors were calculated as $R = (\chi_M T_{exp} - \chi_M T_{calc})2/(\chi_M T_{exp})2$. Excellent fits nicely reproducing the experimental data, including the $\chi_M T$ minima, were obtained for the parameters $J_2 = -71.4$ cm^{-1}, $J_3 = 17.2$ cm^{-1}, g = 2.24 ($R = 3.44 \times 10^{-5}$) for 1, $J_2 = -153$ cm^{-1}, $J_3 = +22$ cm^{-1}, and g = 2.22 ($R = 1.17 \times 10^{-5}$) for 2 and $J_2 = -164$ cm^{-1}, $J_3 = +30$ cm^{-1}, and g = 2.21 ($R = 9.80 \times 10^{-6}$) for 3, Fig. 7.

As was indicated above, one of the Cu–O–Cu bond angles of compound 1 is $\gamma = 108.7°$ and it should be close to the FM-AF limit and consequently with a low absolute value. A second simulation discarding this interaction was performed to prove this assumption applying the simplified Hamiltonian:

$$H = -J_2(S_1 \cdot S_3) - -J_3(S_2 \cdot S_3 + S_2 \cdot S_4) \quad (8)$$

obtaining an equally good fit for the parameters J2 = −64.8 cm^{-1}, $J_3 = 12.8$ cm^{-1}, $g = 2.26$, which probably are more reliable.

The values for the antiferromagnetic interactions are in good agreement with the increase in the largest Cu–O–Cu bond angle of 112.2° for 1, 120.1° for 2 and 124.4° for 3.

Ground state for the three complexes is then $S = 1$, with a 7.5, 29.8 and 30.7 cm^{-1} gap to the first $S = 0$ excited spin level for 1–3 respectively (Fig. 8). As a consequence of this spin level distribution, the magnetization of these complexes must be similar, following an $S = 1$ Brillouin shape. Magnetization experiments performed in the 0–5 T range of an applied external field nicely confirm this assumption, tending in all cases to a quasi saturated magnetization value equivalent to two electrons (Fig. 8).

Comments to the bibliographic data. Overlooked S = 1 cubes

The analysis of the bibliographic data of the magnetic properties of Cu^{II} cubes belonging to the 2 + 4 class, published along more than twenty years, reveals to be extremely confused. Some relevant magnetic features for 43 of those cubanes are summarized in Table 3. In this table the cubes with all of the elongated Cu–O distances larger than an arbitrary value of 2.60 Å (for which negligible magnetic interactions through the elongated opposite faces must be assumed) are tabulated separately. In addition to these 37 complexes, there are six other cubes for which disputable (but relevant) magnetic data were reported, that will be discussed specifically. An overview of the data collected in Table 3 evidences that the models applied in the magnetic analysis are not always justified. For cubes with large elongated Cu–O distances, the most reasonable approach seems to be the one J model (0:4), and effectively, most of these cubes were fitted according this model. However, in spite of the structural evidence, in some few cases the authors assumed the regular cube model (6) (ELEYIE, NILDAP or WEMSUE).

As can be expected, J_1 usually shows low values for all cubes fitted with the (2:4) model and $S = 0$ ground state but in contrast, the large values of J_1 reported for QOMRAL or POLKEH seem to be clearly overestimated. In this sense, the fits performed for LOCPIE and NODHEV become interesting, for which the authors compared the fits with the (2:4) and (0:4) models obtaining minimal deviation in J_2, evidencing that for strongly AF coupled cubes the calculated value for J_1 is poorly reliable.

Much more interesting is the analysis of the models applied for ferromagnetic cubes. These kind of systems can give a $\chi_M T$ plot that suggests the expected value for a $S = 2$ total spin but often, a decay at low temperature or a continuous increase in $\chi_M T$ up to a value slightly lower than the expected for $S = 2$ has been reported. These plot shapes can be due to intercluster interactions or weak anisotropy in the ground state, as has been demonstrated for FEVYAH by Ozarowski et al.[21] When the isotropic (2:4) model was applied to fit cubes with a ferromagnetic response, a systematic error is often produced, that consists of the obtention of a pair of coupling constants with characteristic values very close to $-2J1 = J2$ as occurs for ASUPEJ01, BUFTUR, CAQDAZ, IHELOX, NAXBET, SAPYUE, XOVVUA or XOXGEY. The reason for this can be found in the plot of the spin levels for a ferromagnetic cube in Fig. 4c: for a $-J1/J2 = 0.5$ ratio there is a crossing between the $S = 0$ and the $S = 2$ spin levels and the population of both levels produces a decay of the $\chi_M T$ plot at low temperature (Fig. *S1*†).

The $S = 1$ ground state was erroneously claimed for ASUPEJ01, SAPYOY and SAPYUE despite their $\chi_M T$ plots showing a continuous increase for decreasing temperatures. Fits were performed with the (2:4) model that never can lead to the $S = 1$ ground state and these three cubes are obviously ferromagnetic, with a $S = 2$ ground state.

In contrast, reviewing the $\chi_M T$ plots reported for this kind of cubes, we realized that the $S = 1$ ground state is unusual but not unprecedented. DIBTAL shows a $\chi_M T$ response very similar to that of complex 1 but the authors reported the magnetic properties of this cube as being unexplainable and no fit was tried. From its $\chi_M T$ shape and the low temperature value (with a plateau at around 1.1 $cm^3\ Kmol^{-1}$), the $S = 1$ ground state becomes evident. The reason for this magnetic response lies in their α–δ Cu–O–Cu bond angles which follows the sequence 112.3°–111.2°–99.7°–105.5°, corresponding to the (0:2:2c) model with two ferromagnetic and two antiferromagnetic contiguous interactions.

Other cubes with a probable $S = 1$ ground state are the enantiomers MOYJUH (*R*) and MOYKAO (*S*) recently reported by S. Gao et al.;43 only the (*R*) isomer MOYJUH was measured. Its low temperature $\chi_M T$ plot tends clearly to 1.1 $cm^3\ Kmol^{-1}$and the fit of the experimental data was performed with the (2:4) model discarding the low temperature data. The reported values of $J_1 = -11.2\ cm^{-1}$ and $J_2 = +7.6\ cm^{-1}$ lead to a well defined $S = 0$ ground state with a gap of 11 cm^{-1} to the first $S = 1$ excited level, which is not compatible with the experimental plot. The clearest proof for the $S = 1$ ground state for this compound was provided by its magnetization, which follows an apparent Brillouin shape, tending to the equivalent to two electrons.[43] The α–δ sequence of Cu–O–Cu bond angles for MOYJUH are comprised between 100.5°–107.4° and then does not follow the (0:1:3) nor the (0:2:2c) scheme. However, this compound is extremely unusual because three Cu^{II} cations show a square pyramidal environment whereas the fourth Cu^{II} cation has a trigonal bipyramidal coordination and then a new model and probably DFT calculations would be necessary to explain its unusual magnetic response.

Magneto-structural correlations. Finally, an undesirable consequence of the employment of unreliable J values should be pointed out, which were obtained by applying inappropriate models to fit the experimental data: several trials to correlate the J values with the experimental Cu–O–Cu bond angles[2,11b,c] or more recently, the proposal of Boča et al.[11a] as a basis of a chemometric analysis of the

Cu^{II} chromophores are far from being a linear relationship and partially it is due (as several authors have pointed out) to the employment of unreliable experimental *J* values.

Along the paper we have assumed that the main parameter that determines the magnetic response of the (4 + 2) class of Cu^{II} cubes is the set of four *α–δ* Cu–O–Cu bond angles. To perform a final check of the validity of this very simplified model, we have selected a coherent group of cubes on the basis of the following four conditions: (i) *comparable μ3-OR bridging ligands*. Practically all complexes are linked by alcoxo or phenoxo bridges but complexes as GIBHAC have been excluded because the bridging ligands are μ3-OH, which gives a completely different magnetic response. (ii) S4 or quasi S4 symmetry. It means that the four α–δ Cu–O–Cu bond angles are identical or with a maximum tolerance of ± 1°. (iii) *Square pyramidal or elongated octahedron environment around the four Cu^{II} cations.* It means to discard complexes in which one or more copper atoms have a BPT environment. (iv) *To discard any questionable value* (mainly for the cubes with an S = 2 ground state), indicated in the previous section.

The plot of the unfiltered J_2 values vs. the mean Cu–O–Cu *α–δ* bond angles for all compounds reported in Table 3 is very disperse and no conclusion can be extracted (Fig. 9). However, plotting the 20 selected cubes with the above criteria provides a clear indication of the dependence of the sign of the magnetic interaction with this parameter and corroborates the assumption of the FM/AFM limit around 108°–110°. There are only two cubes BOGCOP and DARKUC that are clearly out of this correlation without any apparent reason.

Conclusions

Three new Cu^{II} cubane-like complexes belonging to the (4 + 2) class have been characterised. From the analysis of the susceptibility and magnetization data, the $S = 1$ ground state has been unambiguously assigned for all of them together with the new coupling schemes that justify this unprecedented response. A detailed analysis of the bibliographic data reveals that, to avoid overparametrization, often oversimplified or inappropriate coupling schemes have been applied leading to a confuse landscape. The reported 1–3 compounds are the first characterized cubes with an $S = 1$ ground state but they are not the first compounds exhibiting this property, because in the literature we have found three unexplained systems that belong to this unusual family.

352 **Acknowledgements**

353 Founds from Ministerio de Economia y Competitividad, Project CTQ2012-30662 are acknowledged.

354

References

R. Mergehenn and W. Haase, Acta Crystallogr., Sect. B: Struct. Sci., 1977, 32, 505.

J. Tercero, E. Ruiz, S. Alvarez, A. Rodriguez-Fortea and P. Alemany, J. Mater. Chem., 2006, 16, 2729.

(a) S.-C. Cheng and H.-H. Wei, Inorg. Chim. Acta, 2002, 340, 105; (b) T. J. Boyle, L. M. Ottley and R. Raymond, J. Coord. Chem., 2010, 63, 545; (c) X.-F. Zhang, Q. Yang, J.-P. Zhao, T.-L. Hu, Z. Chang and X.-H. Bu, Sci. China: Chem., 2011, 54, 1446.

(a) W. Choong and N. C. Stephenson, Cryst. Struct. Commun., 1975, 4, 275; (b) J. Moncol, K. Jomova, L. Zelenicky, T. Lis and M. Valko, Acta Crystallogr., Sect. C: Cryst. Struct. Commun., 2011, 67, m318; (c) X. Zhang, B. Li, J. Tang, J. Tian, G. Huang and J. Zhang, Dalton Trans., 2013, 42, 3308.

(a) H.-M. Lv, S.-N. Wang, D.-C. Li and J.-M. Dou, Acta Crystallogr., Sect. C: Cryst. Struct. Commun., 2014, 70, 843; (b) S.-G. Ang, B.-W. Sun and S. Gao, Inorg. Chem. Commun., 2004, 7, 795.

N. Lah, I. Leban and R. Clerac, Eur. J. Inorg. Chem., 2006, 4888.

(a) T. N. Hooper, J. Schnack, S. Piligkos, M. Evangelisti and E. K. Brechin, Angew. Chem., Int. Ed., 2012, 51, 4633; (b) J.-L. Liu, W.-Q. Lin, Y.-C. Chen, S. Gomez-Coca, E. Ruiz, J.-D. Leng and M.-L. Tong, Chem. – Eur. J., 2013, 19, 17567.

Z.-G. Gu, X.-H. Zhou, Y.-B. Jin, R. G. Xiong, J.-L. Zuo and X.-Z. You, Inorg. Chem., 2007, 46, 5462.

G. M. Sheldrick, Acta Crystallogr., Sect. A: Fundam. Crystallogr., 2008, 64, 112.

Ortep-3 for Windows: L. J. Farrugia, J. Appl. Crystallogr., 1997, 30, 565.

(a) Z. Puterová-Tokárová, V. Mrázová, J. Kožíšek, J. Valentová, B. Vranovičová and R. Boča, Polyhedron, 2014, 70, 52; (b) S. Thakurta, P. Roy, R. J. Butcher, M. S. El Fallah, J. Tercero, E. Garribba and S. Mitra, Eur. J. Inorg. Chem., 2009, 4385; (c) E. Gungor, H. Kara, E. Colacio and A. J. Mota, Eur. J. Inorg. Chem., 2014, 1552.

N. F. Chilton, R. P. Anderson, L. D. Turner, A. Soncini and K. S. Murray, J. Comput. Chem., 2013, 34, 1164.

D. Maity, A. D. Jana, M. Debnath, N. G. R. Hearns, M.-H. Sie, H. M. Lee, R. Clerac and M. Ali, Eur. J. Inorg. Chem., 2010, 3484.

R. Papadakis, E. Riviere, M. Giorgi, H. Jamet, P. Rousselot- Pailley, M. Reglier, A. J. Simaan and T. Tron, Inorg. Chem., 2013, 52, 5824.

B. Abarca, R. Ballesteros, M. Chadlaoui, C. R. de Arellano and J. A. Real, Eur. J. Inorg. Chem., 2007, 4574.

R. Wegner, M. Gottschaldt, H. Gorls, E.-G. Jager and D. Klemm, Chem. – Eur. J., 2001, 7, 2143.

Y.-M. Li, J.-J. Zhang, R.-B. Fu, S.-C. Xiang, T.-L. Sheng, D.-Q. Yuan, X.-H. Huang and X.-T. Wu, Polyhedron, 2006, 25, 1618.

L. Walz, H. Paulus, W. Haase, H. Langhof and F. Nepveu, J. Chem. Soc., Dalton Trans., 1983, 657.

X. S. Tan, Y. Fujii, R. Nukada, M. Mikuriya and Y. Nakano, J. Chem. Soc., Dalton Trans., 1999, 2415.

H. Astheimer, F. Nepveu, L. Walz and W. Haase, J. Chem. Soc., Dalton Trans., 1985, 315.

E. A. Buvaylo, V. N. Kokozay, O. Yu. Vassilyeva, B. W. Skelton, J. Jezierska, L. C. Brunel and A. Ozarowski, Inorg. Chem., 2005, 44, 206.

X. F. Yan, J. Pan, S. R. Li, H. Zhou and Z. Q. Pan, Z. Anorg. Allg. Chem., 2009, 635, 1481.

H. Oshio, Y. Saito and T. Ito, Angew. Chem., Int. Ed. Engl., 1997, 36, 2673.

Z. Lu, T. Fan, W. Guo, J. Lu and C. Fan, Inorg. Chim. Acta, 2013, 400, 191.

C. Aronica, G. Chastanet, G. Pilet, B. Le Guennic, V. Robert, W. Wernsdorfer and D. Luneau, Inorg. Chem., 2007, 46, 6108.

Y. Xie, J. Ni, F. Zheng, Y. Cui, Q. Wang, S. W. Ng and W. Zhu, Cryst. Growth Des., 2009, 9, 118.

N. Chopin, M. Medebielle, O. Maury, G. Novitchi and G. Pilet, Eur. J. Inorg. Chem., 2014, 6185.

P. Bhowmik, N. Aliaga-Alcalde, V. Gomez, M. Corbella and S. Chattopadhyay, Polyhedron, 2013, 49, 269.

W.-H. Gu, X.-Y. Chen, L.-H. Yin, A. Yu, X.-Q. Fu and P. Cheng, Inorg. Chim. Acta, 2004, 357, 4085.

M. Sutradhar, M. V. Kirillova, M. F. C. Guedes da Silva, C.-M. Liu and A. J. L. Pombeiro, Dalton Trans., 2013, 42, 16578.

A. Chakraborty, K. L. Gurunatha, A. Muthulakshmi, S. Dutta, S. K. Pati and T. K. Maji, Dalton Trans., 2012, 41, 5879.
E. Gojon, J. M. Latour, S. J. Greaves, D. C. Povey, V. Ramdas and G. W. Smith, J. Chem. Soc., Dalton Trans., 1990, 2043.
J. Tang, J. S. Costa, A. Pevec, B. Kozlevcar, C. Massera, O. Roubeau, I. Mutikainen, U. Turpeinen, P. Gamez and J. Reedijk, Cryst. Growth Des., 2008, 8, 1005.
J. P. Laurent, J. J. Bonnet, F. Nepveu, H. Astheimer, L. Walz and W. Haase, J. Chem. Soc., Dalton Trans., 1982, 2433.
J. Chakraborty, S. Thakurta, G. Pilet, D. Luneau and S. Mitra, Polyhedron, 2009, 28, 819.
J. P. Costes, C. Duhayon and L. Vendier, Inorg. Chem., 2014, 53, 2181.
C. Maxim, T. D. Pasatoiu, V. Ch. Kravtsov, S. Shova, C. A. Muryn, R. E. P. Winpenny, F. Tuna and M. Andruh, Inorg. Chim. Acta, 2008, 361, 3903.
M.-L. Liu, J.-M. Dou, J.-Z. Cui, D.-C. Li and D.-Q. Wang, J. Mol. Struct., 2012, 1011, 140.
K. H. Whitmire, J. C. Hutchison, A. Gardberg and C. Edwards, Inorg. Chim. Acta, 1999, 294, 153.
S. Banerjee, S. Sen, J. Chakraborty, R. J. Butcher, C. J. Gomez Garcia, R. Puchta and S. Mitra, Aust. J. Chem., 2009, 62, 1614.
A. Mukherjee, R. Raghunathan, M. K. Saha, M. Nethaji, S. Ramasesha and A. R. Chakravarty, Chem. – Eur. J., 2005, 11, 3087.
S.-S. Qian, Y. Zhao, M.-M. Zhen, C.-L. Zhang, Z.-L. You and H.-L. Zhu, Transition Met. Chem., 2013, 38, 63.
Ji Yin, T.-T. Yin, C. Gao, B.-W. Wang, Y.-Y. Zhu, Z.-Q. Wu and S. Gao, Eur. J. Inorg. Chem., 2014, 5385.

Legends to figures

Scheme 1 Schematic drawing of the cubane CuII complexes according the relative position of the elongated Cu–O distances (red dashed bonds).

Scheme 2 Ligands employed in this work and their coordination mode in the {Cu4O4} core of compounds 1–3.

Fig. 1 Top, a view of the molecular structure of compound 1. Bottom, the labeled core of the cubane. Bonds depicted in orange correspond to the short Cu–O distances inside the {Cu4O4} cage

Fig. 2 Top, a view of the molecular structure of compound 2. Bottom, the labeled core of the cubane. Bonds depicted in orange correspond to the short Cu–O distances inside the {Cu4O4} cage

Fig. 3 Top, a view of the molecular structure of compound 3. Bottom, the labeled core of the cubane. Bonds depicted in orange correspond to the short Cu–O distances inside the {Cu4O4} cage and the dashed red bonds show the H-bonds involving the coordinated water molecule

Scheme 3 Interaction schemes for the CuII cubane topology according the literature. The models have been named according to the number of identical faces and coupling constants.

Fig. 4 Plot of the six spin levels of a CuII cubane for: (a) model (0:4) and Hamiltonian (3) for a +25 to −50 cm−1 range of J values, (b) model (2:4) and Hamiltonian (2) for an AF J2, (c) model (2:4) and Hamiltonian (2) for a FM J2 and (d) model (0:2:2) and Hamiltonian (4). Color key of the spin levels: S = 2, red; S = 1, black; S = 0, blue; and degenerate levels, green. Arbitrary value for J2 = −50 cm−1 in (b–d).

Fig. 5 Set of consecutive Cu–O–Co bond angles involving the four short Cu–O distances in the cubane core.

Scheme 4 Low symmetry interaction schemes for the CuII cubane topology proposed for compounds 1–3. The models have been named according to the number of identical faces and coupling constants.

Fig. 6 Plot of the six spin levels of a CuII cubane for the low symmetry models (0:1:3) and Hamiltonian (6) (left) and (2:2:2c) and Hamiltonian (7) (right), showing the S = 1 ground state for J3/J2 ratios lower than −1/3 and 0 respectively. Bottom, the spin arrangement that allows to the S = 1 ground state. Color key of the spin levels: S = 2, red; S = 1, black; S = 0, blue; degenerate levels, green. Arbitrary value for J2 = −50 cm−1.

Fig. 7 Temperature dependence of χMT for compound 1 (circles), 2 (triangles) and 3 (squares). Solid lines show the best obtained fits.

Fig. 8 Left, energy levels calculated from the fit parameters for complexes 1–3. Right, magnetization data for complexes 1 (squares), 2 (circles) and 3 (triangles) in agreement with the expected S = 1 ground state.

Fig. 9 Plot of the relationship between J and the mean α–δ Cu–O–Cu bond angle for all samples tabulated in Table 3 (left) or the 20 selected compounds according the criteria described in the text, (right), (R factor = 0.76). The compounds represented as stars correspond to complexes BOGCOP and DARKUC, which do not follow the correlation

480 **SCHEME** 1

481

482

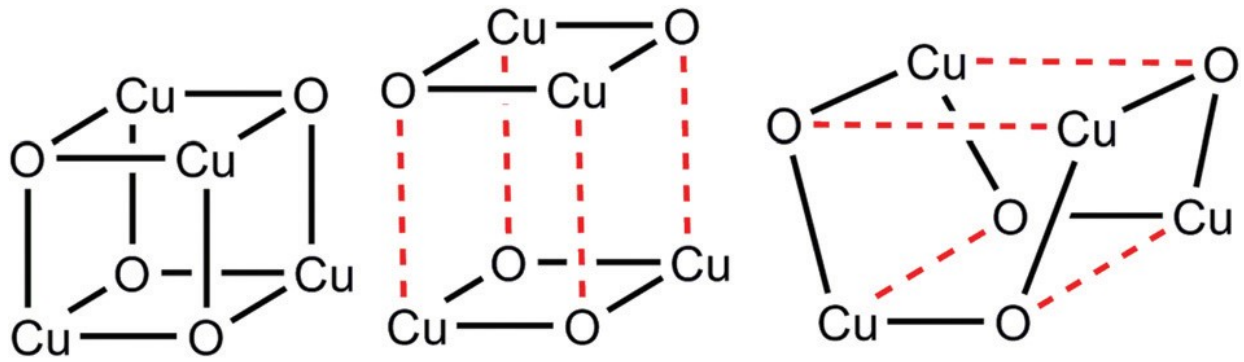

6+0 class **Type I** **2+4 class** **Type II** **4+2 class**

483

484

485 **SCHEME** 2
486
487

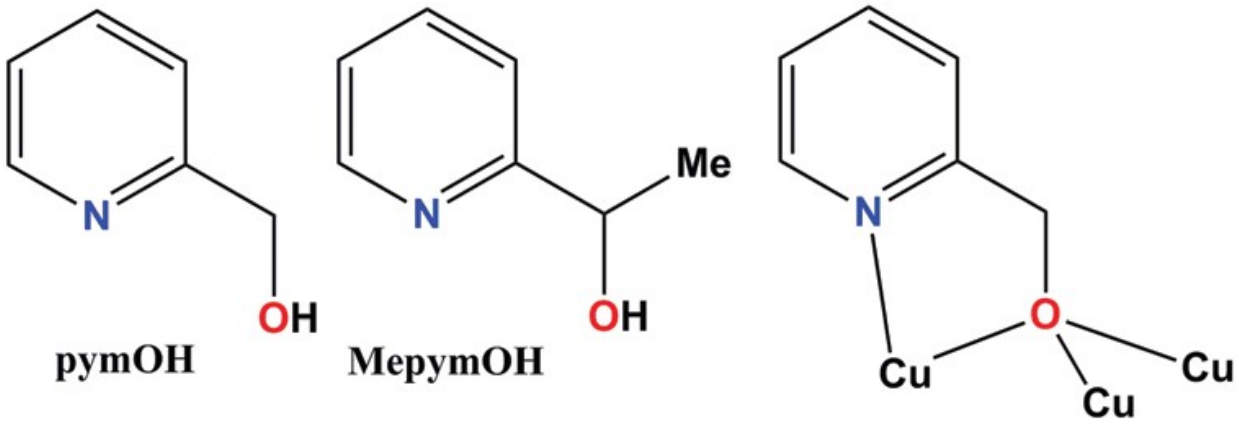

488
489

FIGURE 1

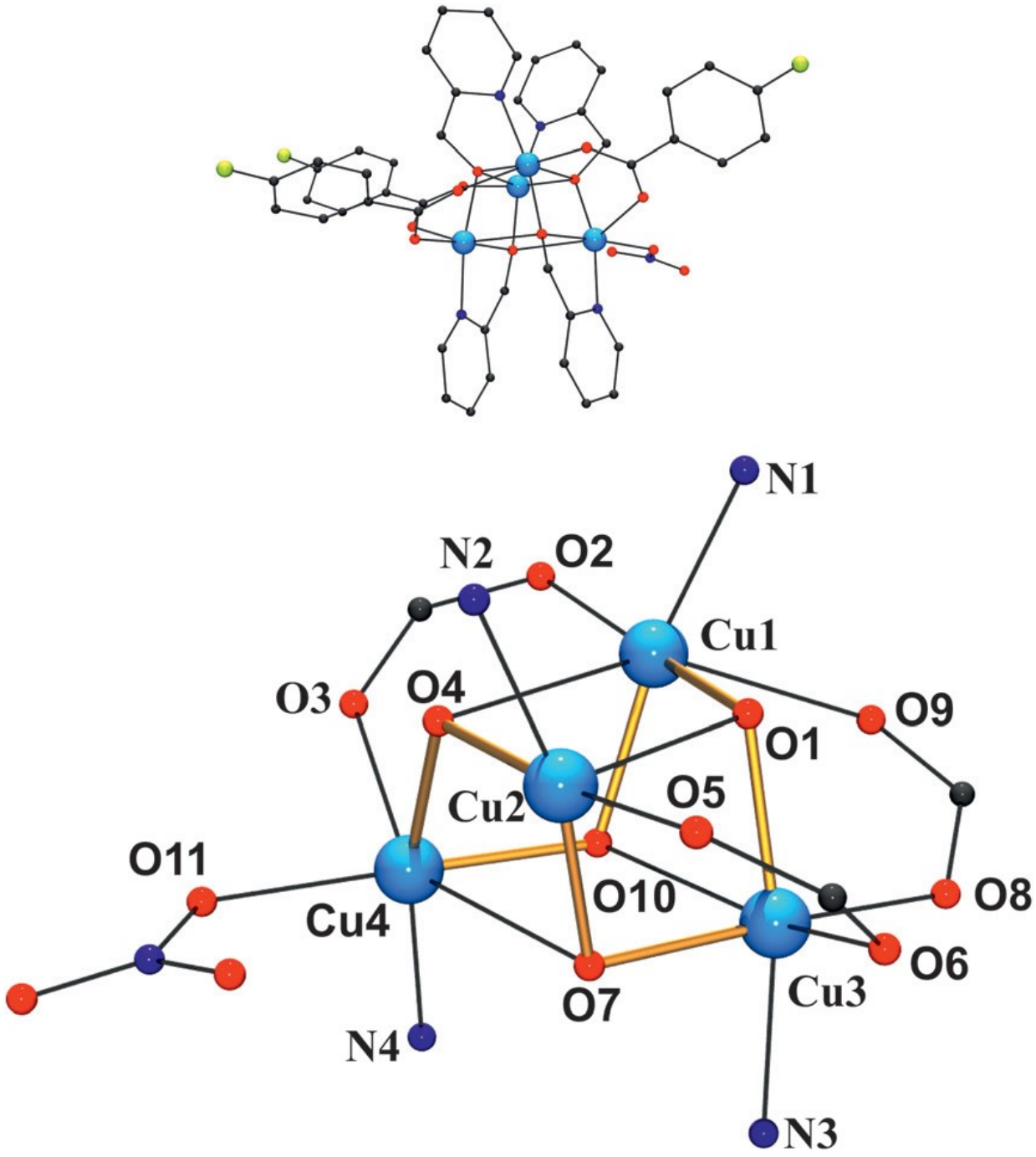

FIGURE 2

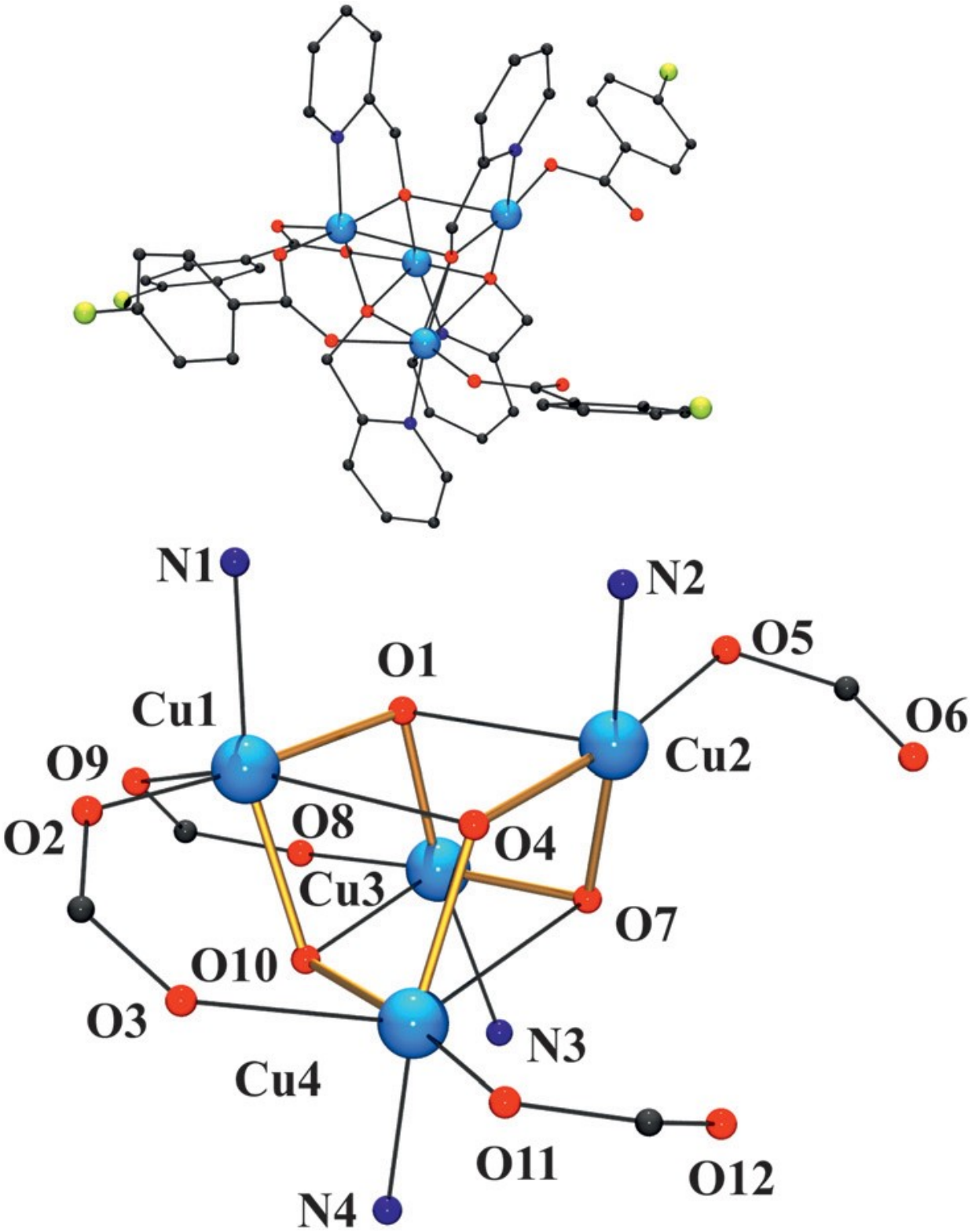

501 **FIGURE** 3

502

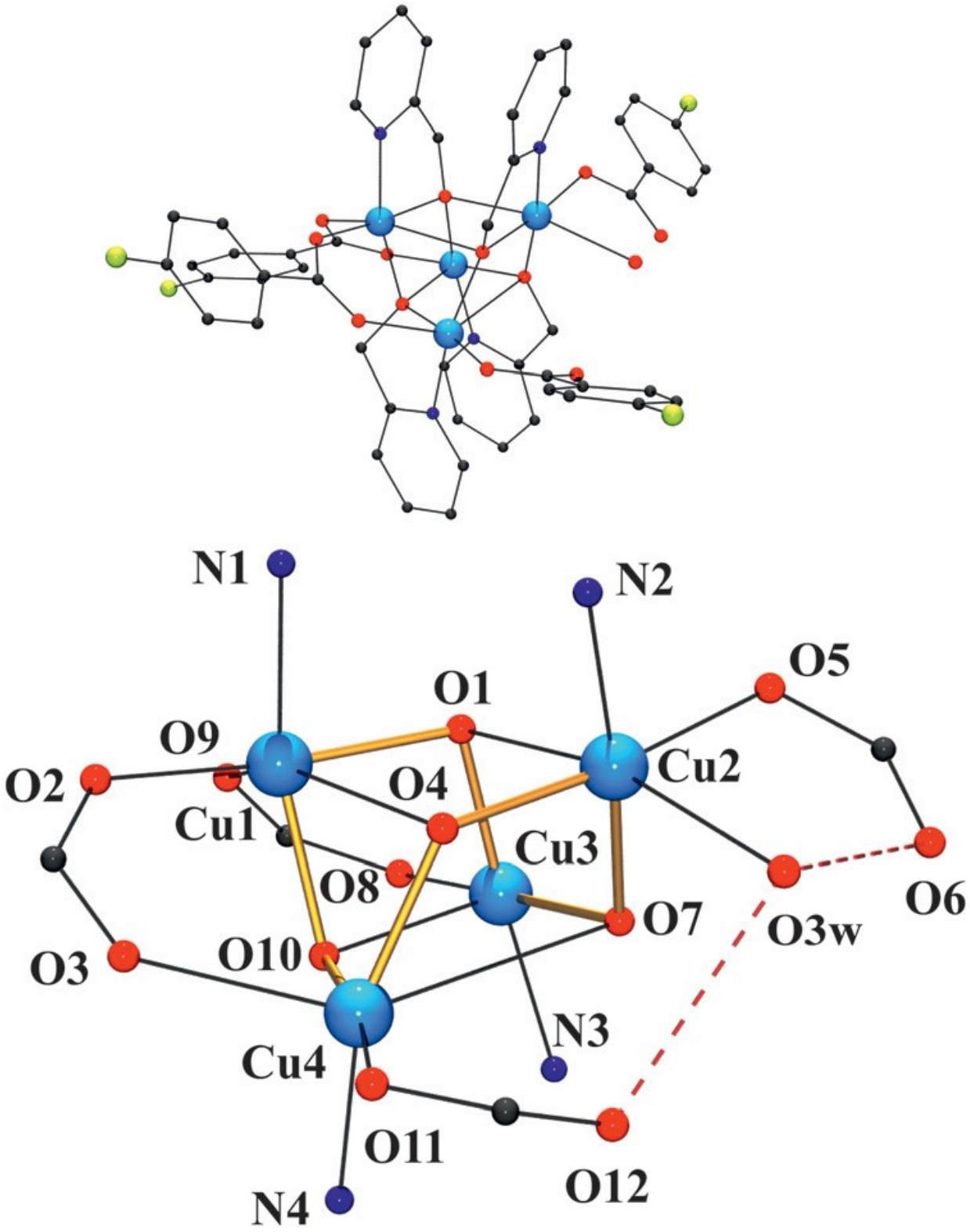

503

504

505 **SCHEME 3**

506

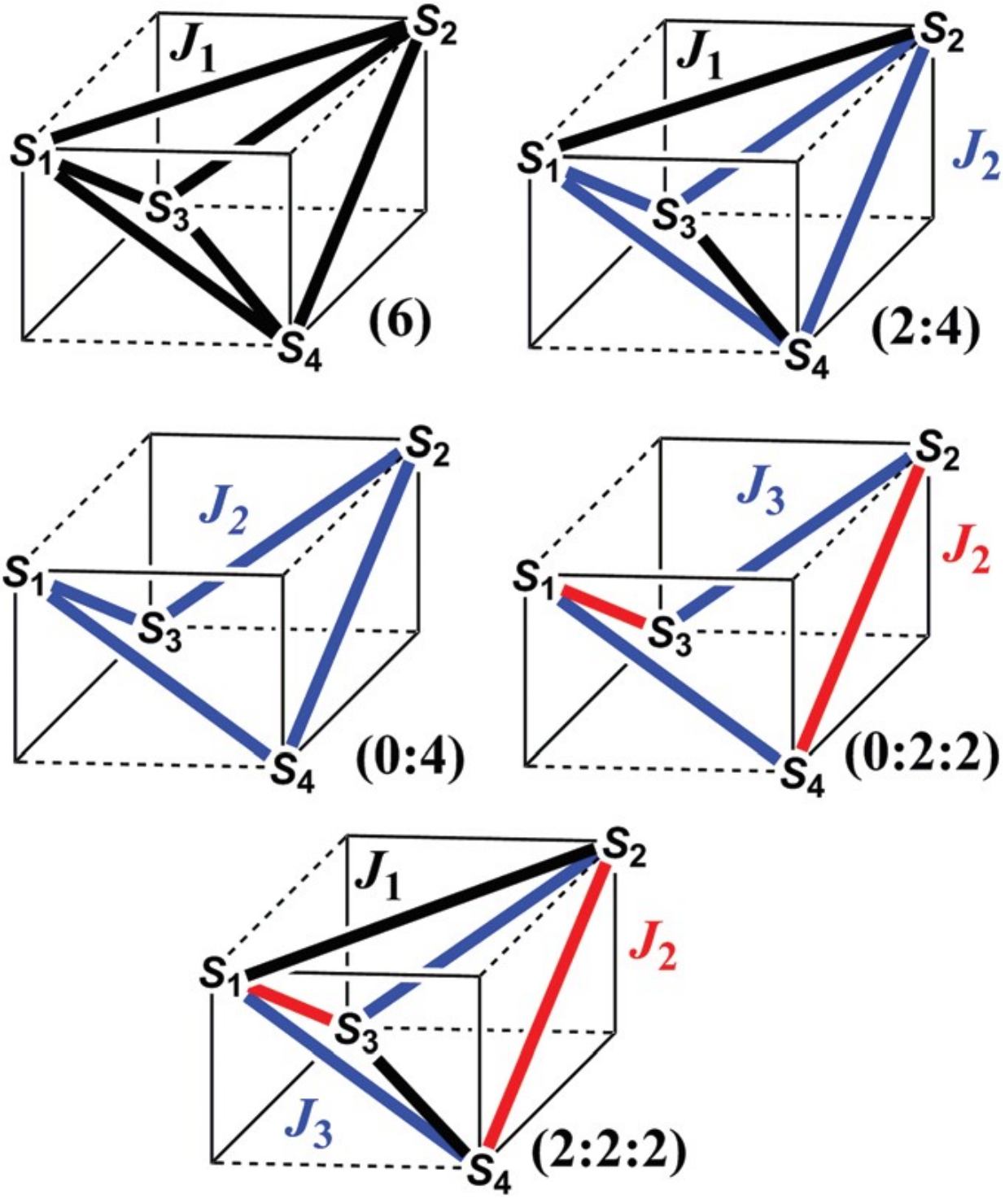

507

508

509

FIGURE 4

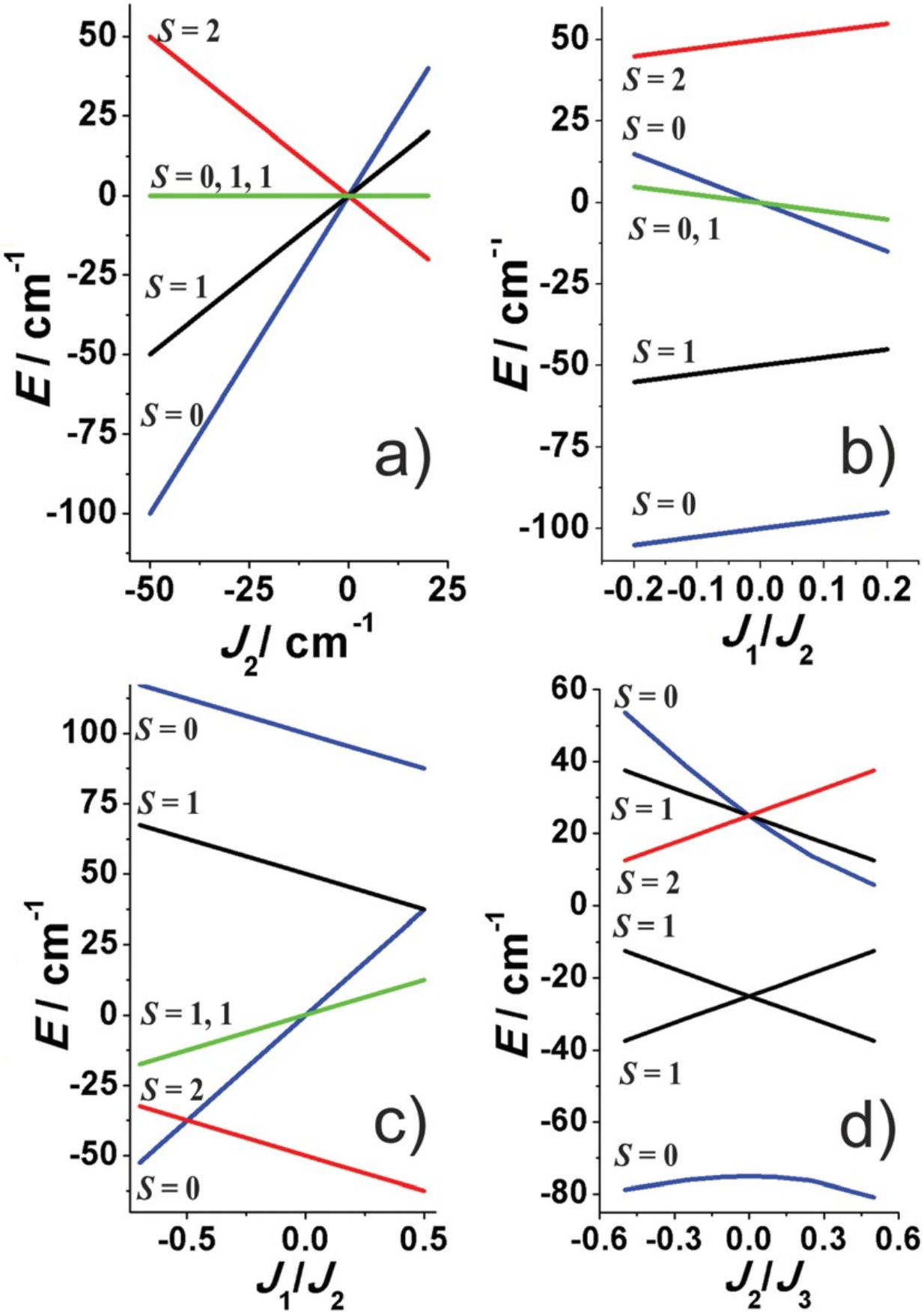

510

511

FIGURE 5

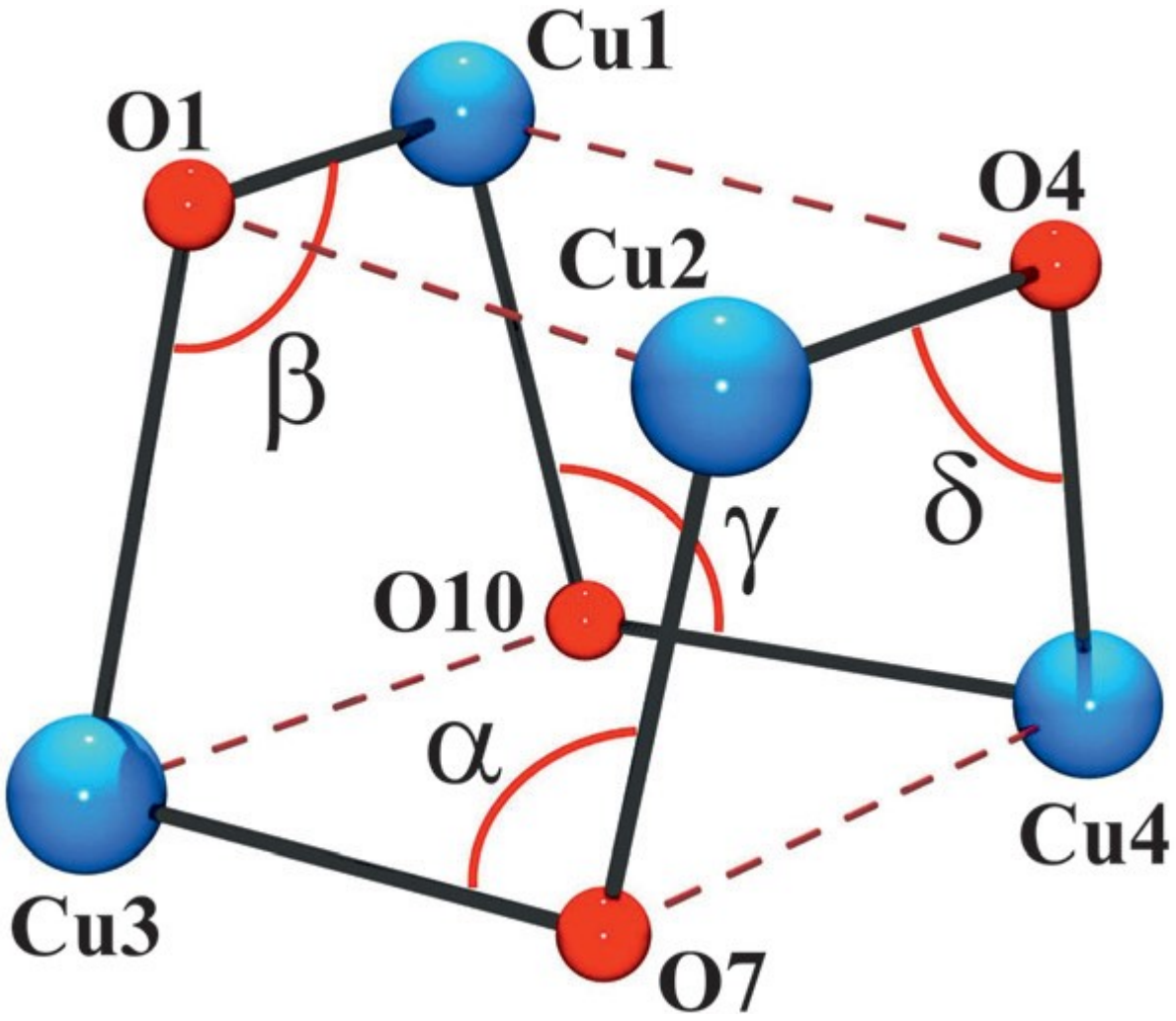

SCEHME 4

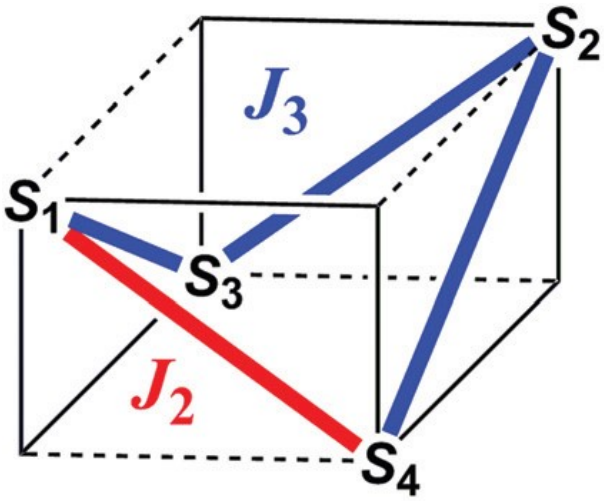

(0:1:3)

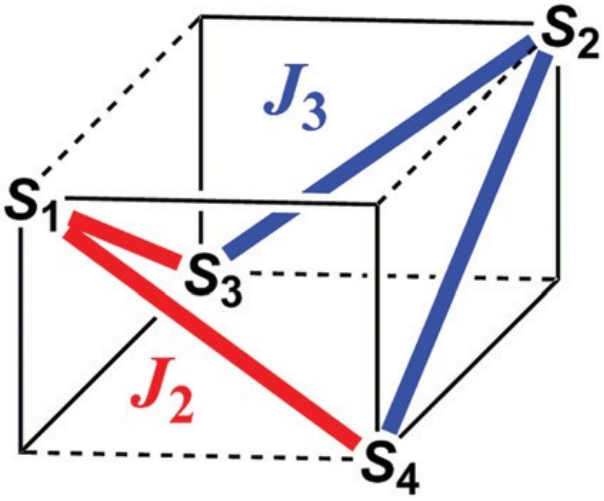

(0:2:2c)

FIGURE 6

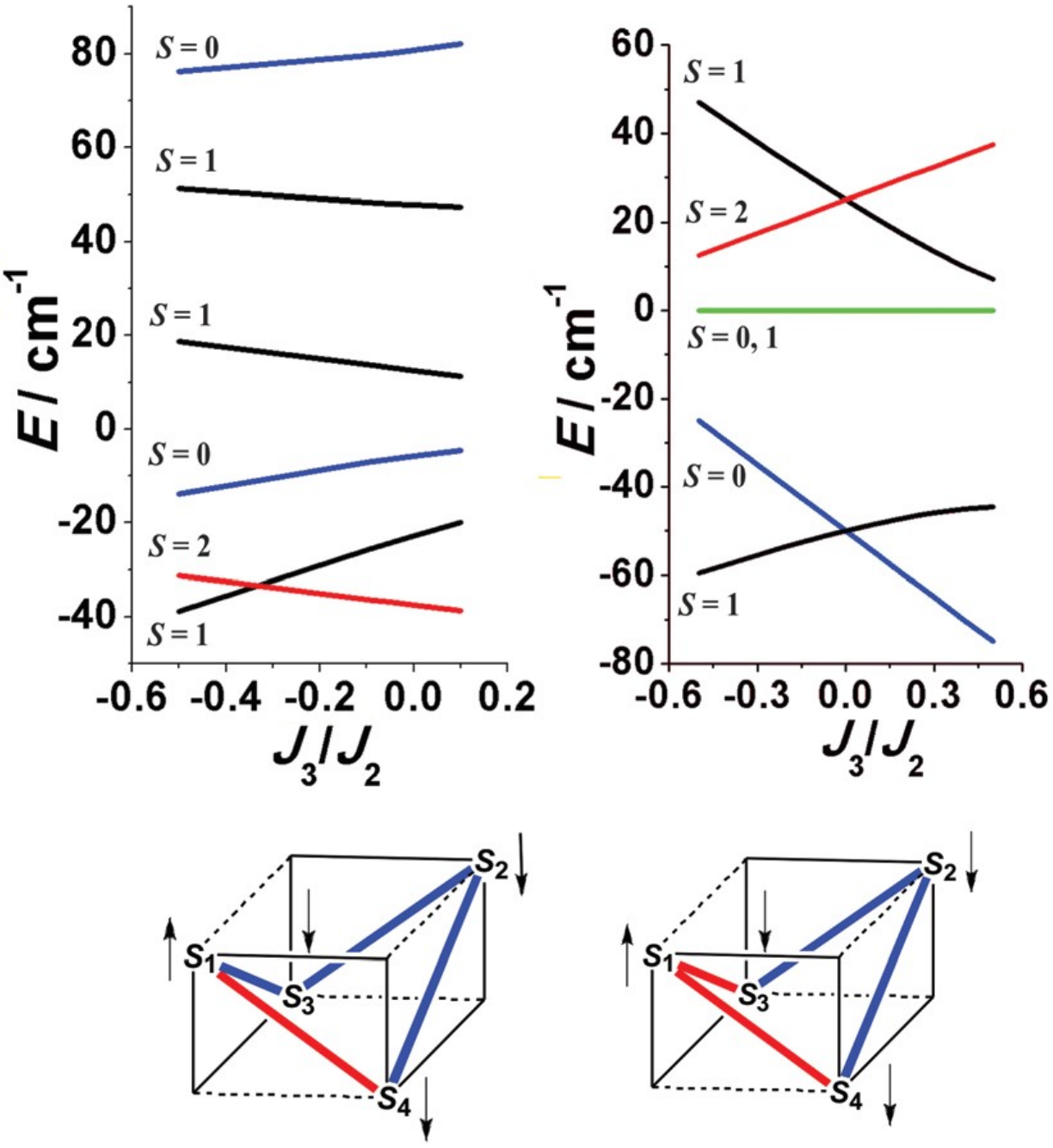
S = 0
S = 1
S = 1
S = 0
S = 2
S = 1
E / cm-1
80
60
40
20
0
-20
-40
-0.6 -0.4 -0.2 0.0 0.2
J3 / J2
S = 1
S = 2
S = 0, 1
S = 0
S = 1
60
40
20
0
-20
-40
-60
-80
-0.6 -0.3 0.0 0.3 0.6
J3 / J2
S1
S2
S3
S4
S1
S2
S3
S4

FIGURE 7

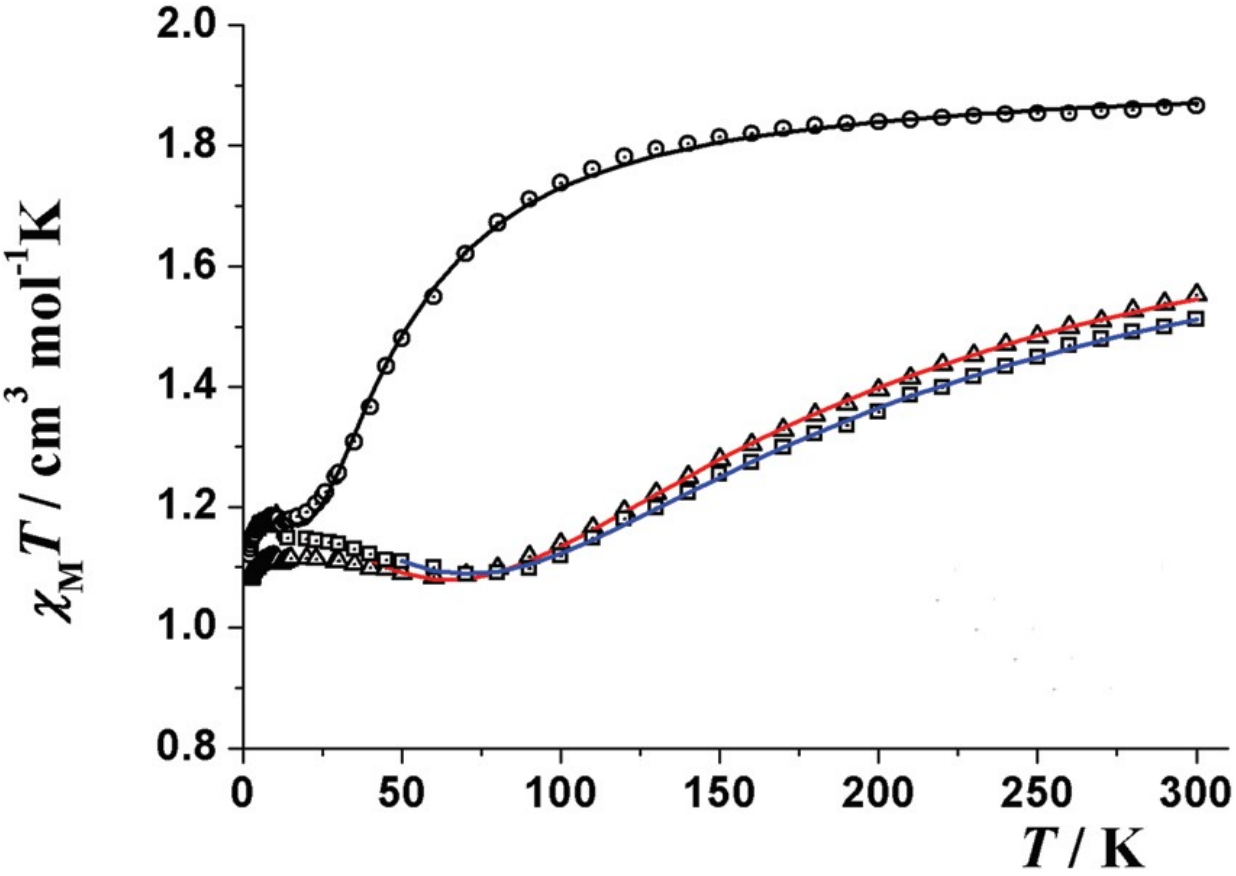

FIGURE 8

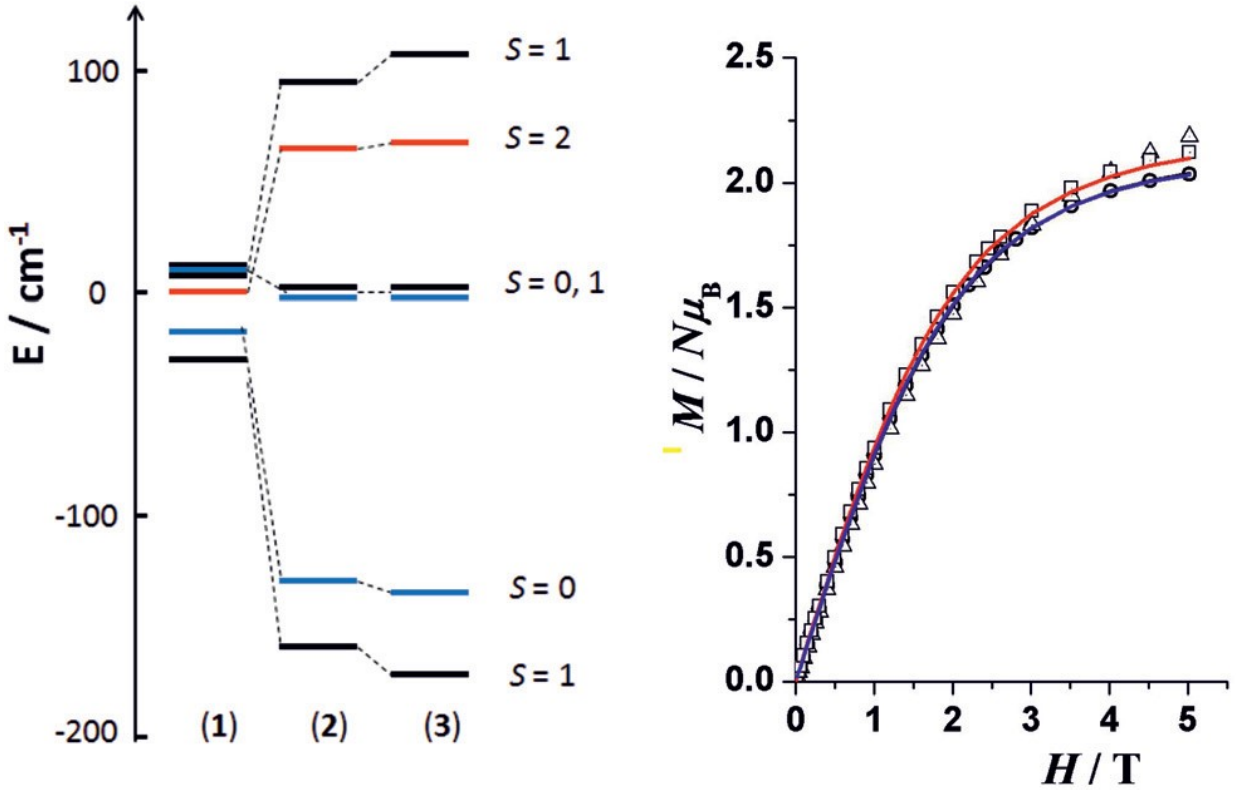
E / cm-1
100
0
-100
-200
(1)
(2)
(3)
S = 1
S = 2
S = 0, 1
S = 0
S = 1
M / Nμ_B
2.5
2.0
1.5
1.0
0.5
0.0
0
1
2
3
4
5
H / T

FIGURE 9

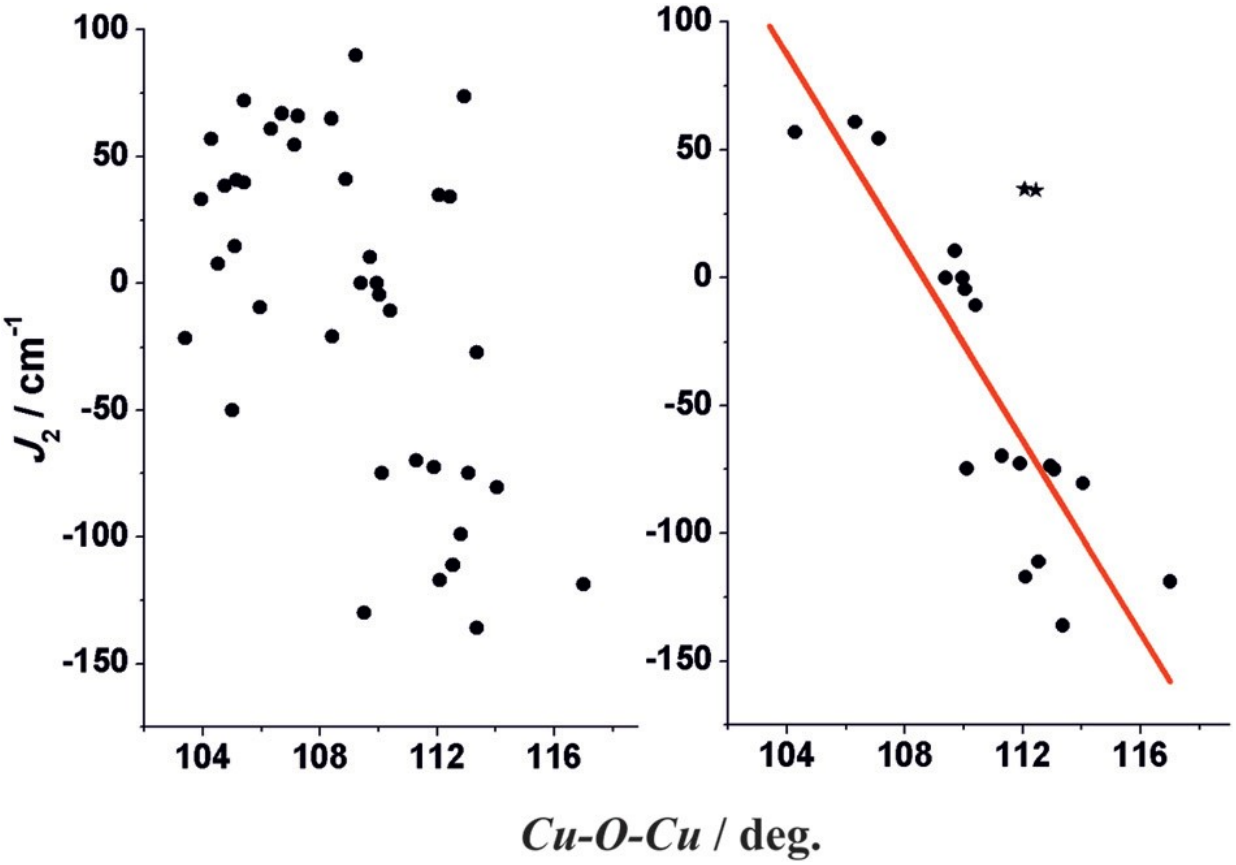

Table 1 Crystal data, collection and structure refinement details for the X-ray structure determination of complexes 1–3

	(1)	(2)	(3)
Formula	$C_{45}H_{36}Cu_4F_3N_5O_{13}$	$C_{52}H_{40}Cu_4F_4N_4O_{12}$	$C_{230}H_{178}Cu_{16}F_{16}N_{16}O_{55}$
F_W	1165.95	1243.04	5126.31
System	Monoclinic	Monoclinic	Monoclinic
Space group	$P2_1/c$	$C2/c$	$C2/c$
a/Å	13.344(13)	38.530(3)	41.241(2)
b/Å	18.937(2)	13.529(11)	13.4071 (6)
c/Å	19.212(16)	19.446(14)	19.5890(9)
α/°	90	90	90
β/°	115.388(5)	92.806(4)	107.999(2)
γ/°	90	90	90
V/Å^3	4385.9(7)	10 125.0(14)	10 301.1(8)
Z	4	8	2
T, K	293(2)	302(2)	100(2)
λ(MoKα), Å	0.71073	0.71073	0.71073
ρ_{calc}, g cm^{-3}	1.766	1.631	1.653
μ(MoK$_\alpha$), mm^{-1}	2.001	1.740	1.715
R	0.0676	0.0485	0.0326
ωR^2	0.1683	0.1265	0.0837

552 **Table 2** Main bond distances (Å) and angles (°) for complexes 1–3

553

Distance Å	(1)	(2)	(3)
Cu1–O1	1.942(2)	1.961(7)	1.969(1)
Cu3–O1	1.983(2)	1.926(7)	1.931(1)
Cu3–O7	1.947(2)	1.929(7)	1.911(1)
Cu2–O7	1.914(2)	1.914(8)	1.948(1)
Cu2–O4	1.916(3)	1.945(6)	1.959(1)
Cu4–O4	1.929(3)	1.931(7)	1.937(1)
Cu4–O10	1.931(2)	1.980(6)	1.980(1)
Cu1–O10	1.922(2)	1.960(7)	1.970(1)
Cu1–O4	2.697(3)	2.651(6)	2.697(1)
Cu2–O1	2.344(3)	2.462(7)	2.417(1)
Cu3–O10	2.410(3)	2.359(6)	2.378(1)
Cu4–O7	2.594(3)	2.962(7)	3.253(1)
Angles (°)	**(1)**	**(2)**	**(3)**
Cu1–O10–Cu4	108.7(1)	104.3(3)	104.23(5)
Cu4–O4–Cu2	112.2(1)	120.1(3)	124.32(6)
Cu2–O7–Cu3	100.3(1)	110.9(4)	110.77(6)
Cu3–O1–Cu1	102.6(1)	101.5(3)	100.80(5)

554

555

556

Table 3 Magnetic data for the (4 + 2) copper cubes reported in the literature. All J values have been normalized to the −JSx·Sy Hamiltonian

CCDC code	Model/ Hamiltonian	$J_1/J_2/J_3$ [a] (cm^{-1})	Ground state	Ref.
Cubes with at least one Jahn–Teller Cu–O distance <2.6 Å				
ELEYIE	(6)/(1)	−20.8	$S = 0$	13
WEMSUE	(6)/(1)	−4.5	$S = 0$	4*c*
GIBHAC	(2:4)/(2)	+7.6/−21.7	$S = 0$	14
NINPEG	(2:4)/(2)	−5.2/−74.8	$S = 0$	15
QOMRAL	(2:4)/(2)	−26/−50	$S = 0$	16
VEGROP	(2:4)/(2)	−6.4/−10.9	$S = 0$	17
BUFTUR	(2:4)/(2)	−19.8/+41.0	$S = 2$	18
CAQDAZ	(2:4)/(2)	−32.6/+89.8	$S = 2$	19
DARKOW	(2:4)/(2)	−14.2/+57.0	$S = 2$	20
FEVYAH	(2:4)/(2)	−1/+65.0	$S = 2$	21
IHELOX	(2:4)/(2)	−31.8/+66.0	$S = 2$	22
LITXOD	(2:4)/(2)	+10.2/+39.8	$S = 2$	11*c*
NAXBET	(2:4)/(2)	−35.2/+72	$S = 2$	23
QOMREP	(2:4)/(2)	+15.2/−9.4	$S = 2$	16
XEXZUX	(2:4)/(2)	−21.4/+54.6	$S = 2$	24
XINYUP	(2:4)/(2)	−10.5/+61.0	$S = 2$	25
XOVVUA	(2:4)/(2)	−33.5/+67.0	$S = 2$	26
XOXGEY	(2:4)/(2)	−20.6/+41.2	$S = 2$	27
FEJMIS	(0:4)/(3)	−99.2	$S = 0$	28
HAKXIB	(0:4)/(3)	+10.4	$S = 2$	29
MUGWUH	(2:2:2)/(5)	+3.0/+24.4/+64.8	$S = 2$	11*b*
WEMTAL	(2:2:2)/(5)	−1.2/−1.2/+74.2	$S = 2$	4*c*
Cubes with all Jahn–Teller Cu–O distances >2.6 Å				
NILDAP	(6)/(1)	−118.8	$S = 0$	30
BAQYAV	(0:4)/(3)	−27.1	$S = 0$	31
JELPUL	(0:4)/(3)	−130.0	$S = 0$	32
UFATOL	(0:4)/(3)	−117.0	$S = 0$	33
UFATUR	(0:4)/(3)	−111.0	$S = 0$	33
BOGCOP	(0:4)/(3)	+34.2	$S = 2$	34
DARKUC	(0:4)/(3)	+34.8	$S = 2$	20
BOQZUD	(2:4)/(2)	+27.2/−69.8	$S = 0$	35
LOCPIE	(0:4)/(2)	−73.6	$S = 0$	36
NODHEV	(2:4)/(2)	+6.2/−80.5	$S = 0$	11*a*
POLKEH	(2:4)/(2)	−46.0/−136.0	$S = 0$	37
VAVGUW	(2:4)/(2)	−5/−75.0	$S = 0$	38
LIJQEA-IE	—	Uncoupled	—	39
GUFJEX01		−72.6	$S = 0$	40
Disputable interesting cases				
ASUPEJ01[a]	(2:4)/(2)	−18/+38.4	$S = 2$	41
SAPYOY[a]	(2:4)/(2)	−18.4/+14.7	$S = 2$	41
SAPYUE[a]	(2:4)/(2)	−15.6/+33.3	$S = 2$	41
DIBTAL[b]	No fit	—	$S = 1$?	42
MOYJUH[b]	(2:4)/(2)	−11.2/+7.6	$S = 1$?	43
MOYKAO[b]			$S = 1$?	43

[a] Complexes for which an $S = 1$ ground state was erroneously assigned.
[b] Complexes that probably have an $S = 1$ ground state.